Pharmaceutical Research, Vol. 27, No. 4, April 2010 (© 2010)
DOI: 10.1007/s11095-009-0047-4

Research Paper

Basolateral Efflux Mediated by Multidrug Resistance-Associated Protein 3 (Mrp3/*Abcc3*) Facilitates Intestinal Absorption of Folates in Mouse

Yoshiaki Kitamura,[1] Hiroyuki Kusuhara,[1] and Yuichi Sugiyama[1,2]

Received October 3, 2009; accepted December 27, 2009; published online February 11, 2010

Purpose. This study investigated the role of an ABC transporter, Mrp3/*Abcc3* in intestinal folate absorption.
Methods. Plasma concentrations of folic acid and leucovorin, given orally, were determined in wild-type and *Mrp3*$^{-/-}$ mice. Mucosal-to-serosal transport was determined in the everted intestinal sacs. The plasma concentrations of endogenous 5-methyltetrahydrofolic acid, homocysteine and vitamin B_{12}, and mRNA levels of hepatic and intestinal folate metabolizing enzymes were compared between wild-type and *Mrp3*$^{-/-}$ mice.
Results. C_{max} and area-under plasma concentration–time curve of folic acid were 3.0- and 2.3-fold lower in *Mrp3*$^{-/-}$ mice compared with wild-type mice, whereas the total body clearance was unchanged. Absorption of leucovorin was significantly delayed in *Mrp3*$^{-/-}$ mice. Mucosal-to-serosal transport of folic acid and leucovorin was significantly decreased in the duodenum of *Mrp3*$^{-/-}$ mice, where their $PS_{serosal}$ was decreased to 6.3 and 22% of that in wild-type mice, respectively. $PS_{serosal}$ of 5-methyltetrahydrofolic acid was moderately decreased in *Mrp3*$^{-/-}$ mice. There was no obvious abnormality in folate homeostasis in *Mrp3*$^{-/-}$ mice.
Conclusions. Mrp3 accounts for the serosal efflux of folic acid and leucovorin, while it makes a moderate contribution to the serosal efflux of 5-methyltetrahydrofolic acid in mice. Mrp3 dysfunction does not disrupt folate homeostasis in mouse.

KEY WORDS: ABC transporters; active transport; intestinal absorption; MRP3; serosal efflux.

INTRODUCTION

Transporters are closely involved in the disposition of nutrients, drugs, and ions, mediating intestinal absorption, tissue distribution and elimination from the systemic circulation. Multidrug resistance-associated protein (Mrp) 3/*Abcc3* belongs to the ATP-binding cassette (ABC) *C* family characterized by the conserved cytosolic domain for ATP binding and hydrolysis. rMrp3 was originally identified as an ABC transporter induced in a mutant rat manifesting jaundice caused by a defect of Mrp2 (1). Mrp3 is expressed on the basolateral membrane of hepatocytes and enterocytes (2,3), and is considered to mediate the efflux of endo- and xenobiotic compounds and their metabolites from cells into the systemic circulation. Recently, the Mrp3 gene was disrupted in mice by homologous recombination to obtain *Mrp3*$^{-/-}$ mice (4). Unlike rats, mouse liver constitutively expresses a significant amount of Mrp3 (4,5), and *Mrp3*$^{-/-}$ mice showed reduced plasma concentrations of morphine-3-glucuronide because of reduced sinusoidal efflux of the glucuronide conjugate formed in the hepatocytes from morphine (4). Reduced sinusoidal efflux causes the enhancement of hepatic elimination from the systemic circulation, unless the uptake is a rate-determining process (6). Actually, the systemic elimination of morphine-6-glucuronide, fexofenadine, and methotrexate was enhanced in *Mrp3*$^{-/-}$ mice compared with wild-type mice (4,7,8).

In addition to the liver, Mrp3 is also expressed on the basolateral membrane of enterocytes (2,9). Considering the membrane localization, Mrp3 can mediate the intestinal absorption of drugs and endogenous compounds. Initially, it was hypothesized that Mrp3 plays a significant role in the enterohepatic circulation of bile acids (10); however, later, it turned out that Mrp3 makes only a negligible contribution to the intestinal absorption of bile acids (2,11,12). We previously reported that Mrp3 is involved in the intestinal absorption of methotrexate. Intrinsic efflux clearance of methotrexate across the basolateral membrane was markedly decreased in *Mrp3*$^{-/-}$ mice, and, thereby, the area under the curve (*AUC*) of the plasma concentrations of methotrexate is lower in *Mrp3*$^{-/-}$ mice compared with wild-type mice (7).

[1] Laboratory of Molecular Pharmacokinetics, Graduate School of Pharmaceutical Sciences, The University of Tokyo, 7-3-1 Hongo, Bunkyo-ku, Tokyo, 113-0033, Japan.
[2] To whom correspondence should be addressed. (e-mail: sugiyama@mol.f.u-tokyo.ac.jp)

ABBREVIATIONS: 5MeTHF, 5-methyltetrahydrofolic acid; ABC, ATP-binding cassette; BLMV, basolateral membrane vesicle; BCRP, breast cancer resistance protein; LC/MS/MS, liquid chromatography/tandem mass spectrometry; MRP, multidrug resistance-associated protein; PCFT, proton-coupled folate transporter; RFC, reduced folate carrier; THF, tetrahydrofolic acid.

In the present study, we report the role of Mrp3 in the absorption of folates in the intestine. Folic acid and leucovorin are known as Mrp3 substrate (13), and the amount of Mrp3 mRNA in the small intestine of mice fed on a folate-deficient diet for eight weeks was enormously increased (14). Folic acid is a water-soluble vitamin (vitamin B_9) which is converted to 5-methyltetrahydrofolic acid (5MeTHF), the principal folate congener supplied to cells as a methyl group donor for the synthesis of amino acids and nucleic acids. The importance of the trans-epithelial transport in intestinal absorption is suggested by the clinical evidence that a loss-of-function mutation of PCFT/*SLC46A1*, a proton-coupled folate uptake transporter on the brush border membrane, is associated with hereditary folate malabsorption (15). The subsequent efflux across the basolateral membrane of folic acid was characterized using membrane vesicles (BLMVs) from rat jejunum and human colon (16,17). The uptake of folic acid by BLMVs from rat jejunum and human colon is saturable and characterized by electroneutral and Na^+-independent uptake and inhibition by a typical inhibitor of anion exchange, 4,4'-di-isothiocyanatostilbene-2,2'-disulphonic acid as well as folate analogs (16,17). However, the involvement of primary active transport has not been examined yet.

In the present study, to elucidate the role of Mrp3 in the intestinal absorption of folic acid, the impact of a defect of Mrp3 on the disposition of folic acid was examined *in vivo* by comparing the plasma concentrations of folic acid in wild-type and *Mrp3*$^{-/-}$ mice, and *in vitro* by comparing the mucosal-to-serosal transport of folic acid, leucovorin, and 5MeTHF in everted sacs from the duodenum where mucosal-to-serosal transport of folates was clearly observed.

MATERIALS AND METHODS

Chemicals and Reagents

Folic acid, leucovorin, and 5MeTHF were purchased from Wako Pure Chemical Industries, Ltd. (Osaka, Japan), Dr. B. Schircks Laboratories (Jona, Switzerland), and Sigma-Aldrich (St Louis, MO), respectively. All other chemicals were commercially available, reagent-grade products.

Animals

Male *Mrp3*$^{-/-}$ (4) and wild-type FVB mice (10–18 weeks old) were used. All animals were kept under standard conditions with a dark–light cycle (12 h–12 h) and were treated humanely. Food and water were available *ad libitum*. The studies were carried out in accordance with the guidelines of the Institutional Animal Care Committee (Graduate School of Pharmaceutical Sciences, The University of Tokyo, Tokyo, Japan).

In Vivo Pharmacokinetic Analysis of Folates in *Mrp3*$^{-/-}$ Mice

Wild-type and *Mrp3*$^{-/-}$ mice were given folic acid (2.3 μmol/kg) and leucovorin (2.0 μmol/kg) orally, dissolved in 100 mM phosphate buffer (pH 7.0) containing 2% ascorbic acid. Blood (about 30 μL) was taken from the tail artery at 0.5, 1, 1.5, 2, 3, and 4 h after administration. In another set of studies, wild-type and *Mrp3*$^{-/-}$ mice received folic acid by constant intravenous infusion at a rate of 2.3 μmol/h/kg. Blood (about 30 μL) was taken from the jugular vein at 30, 60, and 90 min. After oral administration, the peak plasma concentration (C_{max}) was determined by the inspection of individual plasma concentration–time curves. The area under the plasma concentration–time curve (AUC) was calculated by the linear trapezoidal rule up to 4 h. Under the steady-state conditions achieved with the constant intravenous infusion, the total body clearance based on the plasma concentrations ($CL_{tot,p}$) was calculated by dividing the infusion rate by the plasma concentration at steady state (C_{ss}).

Mucosal-to-Serosal Transport of Folates in Everted Sacs From Intestines

The mucosal-to-serosal transport of folates (folic acid, leucovorin, and 5MeTHF) in everted sacs from mouse intestines was determined as reported previously (18). Krebs–Ringer bicarbonate buffer (118 mM NaCl, 4.7 mM KCl, 2.5 mM $CaCl_2$, 1.2 mM KH_2PO_4, 1.2 mM $MgSO_4$, 25 mM $NaHCO_3$, and 11 mM D-glucose, pH 6.8) was used. The duodena (1–8 cm from the stomach) and jejuna (10–18 cm from the stomach) of the wild-type and *Mrp3*$^{-/-}$ mice were excised, trimmed to 6 cm, turned inside out, and immersed in the mucosal buffer (50 mL, 37°C) aerated with 95% O_2+5% CO_2. Serosal buffer was perfused through the everted bowels at 100 μL/min. After 15 min of preincubation, one type of folate was added to the mucosal buffer to a final concentration of 5 μM, and the total volume of the perfused serosal buffer was collected every 10 min. The transport rate in the mucosal-to-serosal direction was calculated by multiplying the concentration in the perfusate by the flow rate. The permeability-surface area products for the net permeation from the mucosal side to the serosal side (PS_{net}) and for the intrinsic efflux transport across the serosal membrane ($PS_{serosal}$) were calculated by dividing the transport rate at 40–50 min in the mucosal-to-serosal direction by the concentration of folate in the mucosal medium (5 μM) and by the concentration in the everted sac tissue (C_{sac}), respectively.

Plasma Levels of Endogenous 5MeTHF, Homocysteine, and Vitamin B_{12}

The plasma 5MeTHF concentration was determined by liquid chromatography/tandem mass spectrometry (LC/MS/MS), and the unbound concentration was measured by ultrafiltration with a micropartition system (MPS-3; Amicon, Danvers, MA). Plasma homocysteine was measured as follows. Plasma specimens were diluted with four volumes of 2.5 mM EDTA. The thiol moiety of the homocysteine was reduced by reacting the diluted plasma (20 μL) with 4 mM dithioerythritol (20 μL) at 37°C for 10 min. Then, 60 μL of 4-(aminosulfonyl)-7-fluoro-2,1,3-benzoxadiazole (0.2 mg/mL) was added, and the sample was incubated at 60°C for 20 min. Finally, 100 μL of 0.3 N perchloric acid was added, and the sample was centrifuged. The supernatant was applied to a high-performance liquid chromatography (HPLC) with a fluorescence detector (excitation 375 nm, emission 510 nm). Plasma vitamin B_{12}

was determined with the Access Vitamin B_{12} assay kit (Beckman Coulter, Inc., Fullerton, CA).

LC/MS/MS and LC/MS Analysis

The plasma concentrations of the folates were determined by LC/MS/MS. For folic acid, the plasma specimens were mixed with an equal volume of 10% trichloroacetic acid/0.1 N hydrochloric acid to deproteinize them. After centrifugation, the supernatant was diluted five-fold with 2% ascorbic acid, and a 30 μL aliquot was injected into the LC/MS/MS system. The detection limit was 2.3 nM, and the calibration curve was linear up to 2,300 nM. For leucovorin, the plasma specimens were mixed vigorously with two volumes of methanol and left on ice for 30 min to deproteinize. After centrifugation, the supernatant was diluted five-fold with water, and a 30 μL aliquot was applied to the LC/MS/MS system. The detection limit was 2.0 nM, and the calibration curve was linear up to 2,000 nM. For 5MeTHF, the plasma specimens (10 μL) were mixed with 1 μL of 1% ascorbic acid and 10 μL of 1.5 M perchloric acid and left on ice for 5 min to deproteinize. After centrifugation, the supernatant (14 μL) was mixed with 2 μL of 8 M potassium acetate and left on ice for 2 min. After centrifugation, the supernatant was diluted five-fold with 2% ascorbic acid, and a 25 μL aliquot was subjected to the LC/MS/MS analysis. The detection limit was 20 nM, and the calibration curve was linear up to 2,000 nM.

In the everted sac study, the concentrations of the folates were determined by LC/MS or LC/MS/MS. For folic acid and leucovorin, serosal buffer samples were centrifuged, and the supernatant (10 μL) was injected into the LC/MS system. Tissue samples were homogenized with nine volumes of methanol, the supernatant of the homogenate was diluted three-fold with water, and a 25 μL aliquot (for folic acid) or a 10 μL aliquot (for leucovorin) was injected into the LC/MS system. The detection limit was 1 nM, and the calibration curve was linear up to 1,000 nM for buffer samples. For 5MeTHF, the buffer samples were diluted five-fold with 2% ascorbic acid and centrifuged. The supernatant (25 μL) was injected into the LC/MS system. Tissue samples were homogenized with nine volumes of methanol, the supernatant of the homogenate was diluted ten-fold with 2% ascorbic acid, and a 50 μL aliquot was applied to the LC/MS/MS system. The detection limit was 1 nM, and the calibration curve was linear up to 1,000 nM for buffer samples.

In the LC/MS analysis, HPLC separation was conducted with a Waters 1525μ Binary HPLC Pump (Waters, Milford, MA) with an L-column ODS (2.1×150 mm, 5 μm; Chemicals Evaluation and Research Institute, Tokyo, Japan). The composition of the mobile phase was acetonitrile/0.05% formic acid (10:90, 10:90, and 6.5:93.5 for folic acid, leucovorin, and 5MeTHF, respectively). The flow rate was 0.3 mL/min. The mass spectra were determined using a Micromass ZQ2000 mass spectrometer (Waters) with the electrospray ionization interface in the selected ion recording (SIR) mode using positive ions m/z 442.0, 474.0, and 460.0 for folic acid, leucovorin, and 5MeTHF, respectively. In the LC/MS/MS analysis, HPLC separation was conducted with a Waters Alliance 2795 Separations Module (Waters). The analytical column, the composition of the mobile phase, and the flow rate were the same as the LC/MS analysis. The mass spectra were determined using a Micromass Quattro Ultima Pt (Waters) with an electrospray ionization interface in the multiple reaction monitoring (MRM) mode using the ion pairs m/z 442.0>295.0, 474.0>327.0, and 460.0>313.0 for folic acid, leucovorin, and 5MeTHF, respectively.

Quantification of mRNA to Assess Folate Homeostasis

Total RNA was prepared from the livers, kidneys, duodena (1–8 cm from the stomach), jejuna (10–18 cm from the stomach), ilea (8 cm above the cecum), and colons (7 cm below the cecum) of wild-type and *Mrp3*$^{-/-}$ mice using ISOGEN (Wako Pure Chemical Industries, Ltd.). After DNaseI treatment (Takara Bio Inc., Otsu, Japan), the RNA was reverse transcribed to single-stranded cDNA using a TaKaRa RNA PCR Kit (AMV) ver. 3.0 (Takara Bio Inc.). Applied Biosystems (Foster City, CA) inventoried TaqMan gene expression assays, which were used to quantify the mRNA levels of dihydrofolate reductase (Dhfr, GenBank no. NM_010049, assay ID Mm00515662_m1), folylpolyglutamyl synthetase (Fpgs, NM_010236, Mm00802614_m1), gamma-glutamyl hydrolase (Ggh, NM_010281, Mm00494593_m1), 5,10-methylenetetrahydrofolate reductase (Mthfr, NM_010840, Mm00487784_m1), serine hydroxymethyltransferase 1 (Shmt1, NM_009171, Mm00486110_m1), and glyceraldehyde-3-phosphate dehydrogenase (Gapdh, NM_008084, Mm99999915_g1).

For the real-time PCR, the TaqMan One-Step Real-Time PCR Master Mix Reagents Kit (Applied Biosystems) containing 900 nM forward primer, 900 nM reverse primer, and 250 nM TaqMan probe was used at 15 μL/well. The Real-Time PCR assay was performed with the 7500 Real-Time PCR System (Applied Biosystems) with the following profile: 50°C for 2 min, 95°C for 10 min, and 40 cycles at 95°C for 15 s and 60°C for 1 min. An external standard curve was generated by dilution of the target PCR product, which was purified by agarose gel electrophoresis (NuSieve GTG Agarose, Lonza, Rockland, ME). All gene expression was normalized to the expression of Gapdh mRNA.

Statistical Analysis

All data represent at least three independent experiments and are expressed as means±standard deviations (SD). Statistically significant differences in the means were assessed using a two-tailed Student's t test. $P<0.05$ was considered statistically significant.

RESULTS

Plasma Concentration–Time Profiles for Folic Acid and Leucovorin in Wild-Type and *Mrp3*$^{-/-}$ Mice

The plasma concentrations of folic acid following its oral administration were determined in wild-type and *Mrp3*$^{-/-}$ mice. They were lower in *Mrp3*$^{-/-}$ mice than in wild-type mice, although this difference was statistically significant at only one point (Fig. 1A). However, both C_{max} and AUC were significantly lower in the *Mrp3*$^{-/-}$ mice than in the wild-type mice (Table I). Folic acid was also given by constant intravenous infusion to wild-type and *Mrp3*$^{-/-}$ mice to determine the total body clearance under steady-state conditions (Fig. 1B). *Mrp3*$^{-/-}$ mice showed similar total

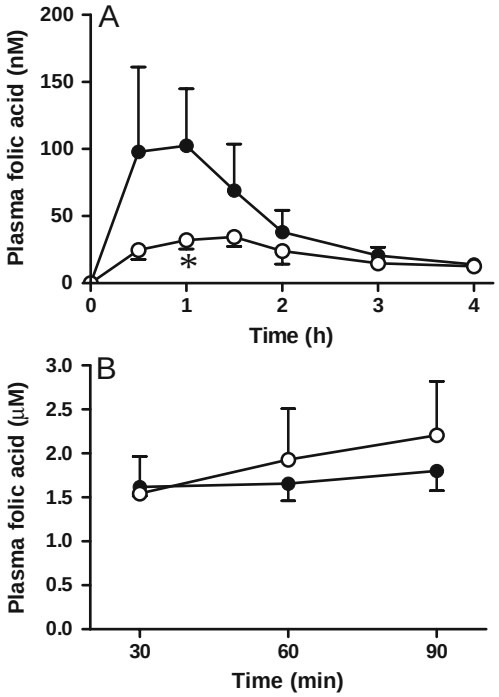

Fig. 1. Time profiles of the plasma concentrations of folic acid in wild-type and *Mrp3*$^{-/-}$ mice following its oral and intravenous administration. Folic acid was given orally to wild-type (*filled circle*) and *Mrp3*$^{-/-}$ (*white circle*) mice at a dose of 2.3 μmol/kg (A) or by a constant intravenous infusion at a rate of 2.3 μmol/h/kg (B). The plasma concentrations were determined at the designated times. Each point represents the mean±SD (n=3 or 4). *P<0.05, significantly different from the wild-type mice.

body clearance to that observed in the wild-type mice (Table I). The plasma concentrations of leucovorin following its oral administration are shown in Fig. 2. The plasma concentrations of leucovorin were significantly lower in the *Mrp3*$^{-/-}$ mice at 0.5 and 1 h after its administration (Fig. 2), although neither C_{max} nor AUC values showed any difference for leucovorin (Table I).

Table I. Pharmacokinetic Parameters of Folates Given by Oral Administration or Intravenous Infusion to Wild-type and *Mrp3*$^{-/-}$ Mice

		Wild-type	*Mrp3*$^{-/-}$
Folic acid			
Oral administration			
C_{max}	nM	110±50	36.4±5.5*
AUC	nM·h	191±80	84.5±4.7*
Intravenous infusion			
C_{ss}	μM	1.80±0.23	2.21±0.61
$CL_{tot,p}$	mL/min/kg	21.2±2.7	17.9±4.4
Leucovorin			
Oral administration			
C_{max}	nM	154±22	123±13
AUC	nM·h	370±28	306±45

Wild-type and *Mrp3*$^{-/-}$ mice were given folic acid (2.3 μmol/kg) or leucovorin (2.0 μmol/kg) orally, or received folic acid by constant intravenous infusion (2.3 μmol/h/kg). The details of the pharmacokinetic analyses are described in Materials and Methods. Each value represents the mean±SD (n=3 or 4). *P<0.05, significantly different from the wild-type mice.

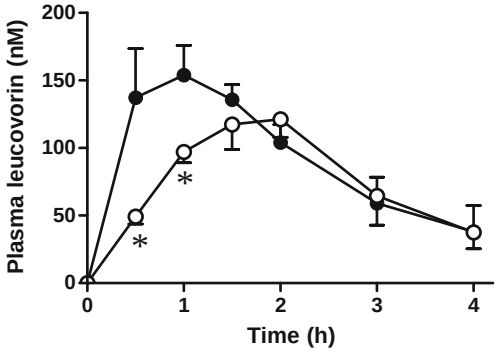

Fig. 2. Time profiles of the plasma concentrations of leucovorin in wild-type and *Mrp3*$^{-/-}$ mice following its oral administration. Leucovorin (2.0 μmol/kg) was given orally to wild-type (*filled circle*) and *Mrp3*$^{-/-}$ (*white circle*) mice. The plasma concentrations were determined at the designated times. Each point represents the mean± SD (n=3). *P<0.05, significantly different from the wild-type mice.

Intestinal Transport of Folates in Everted Sacs

The mucosal-to-serosal transport of folates was determined *in vitro* using everted intestinal sacs prepared from the duodenum and jejunum of wild-type and *Mrp3*$^{-/-}$ mice (Fig. 3, Table II). The permeability–surface area product of the net folic acid transport from the mucosal side to the serosal side (PS_{net}) was significantly lower in the duodenal everted sacs from *Mrp3*$^{-/-}$ mice compared with those from wild-type mice. Considering the 4.0-fold higher concentration of folic acid in the tissues (C_{sac}) of *Mrp3*$^{-/-}$ mice relative to that in wild-type mice, the intrinsic serosal (basolateral) efflux clearance ($PS_{serosal}$) in the *Mrp3*$^{-/-}$ mice was reduced to 6.3% in the duodenum compared with that in the wild-type mice (P<0.05). For leucovorin, the PS_{net} was significantly lower in the duodenal everted sacs from *Mrp3*$^{-/-}$ mice than in those from the wild-type mice. C_{sac} was 2.7-fold higher in *Mrp3*$^{-/-}$ mice than in wild-type mice, and, thus, $PS_{serosal}$ in *Mrp3*$^{-/-}$ mice was about 20% of that in wild-type mice (P<0.05) in the duodenum. PS_{net} and $PS_{serosal}$ of 5MeTHF were also significantly lower in the duodenal everted sacs from *Mrp3*$^{-/-}$ mice than in those from wild-type mice, although the effect of Mrp3 dysfunction was moderate. Unlike the duodenal everted sacs, the jejunal everted sacs showed no differences in PS_{net} or C_{sac} for folic acid or leucovorin between the wild-type and *Mrp3*$^{-/-}$ mice.

Plasma Concentrations of Endogenous 5MeTHF, Homocysteine, and Vitamin B_{12}

There were no differences in the plasma concentrations of endogenous 5MeTHF, homocysteine, or vitamin B_{12} between wild-type and *Mrp3*$^{-/-}$ mice (Fig. 4). The concentrations of unbound 5MeTHF in the plasma were also determined, with similar values in both strains (48.5± 7.3 nM in wild-type and 55.6 ± 12.5 nM in *Mrp3*$^{-/-}$ mice).

Comparison of mRNA Expression Levels of Enzymes Involved in Folate Homeostasis in Wild-Type and *Mrp3*$^{-/-}$ Mice

Hepatic, renal, and intestinal mRNA expression of Dhfr, Fpgs, Ggh, Mthfr, and Shmt1 was quantified in wild-type and *Mrp3*$^{-/-}$ mice (Fig. 5). There was no marked difference in the

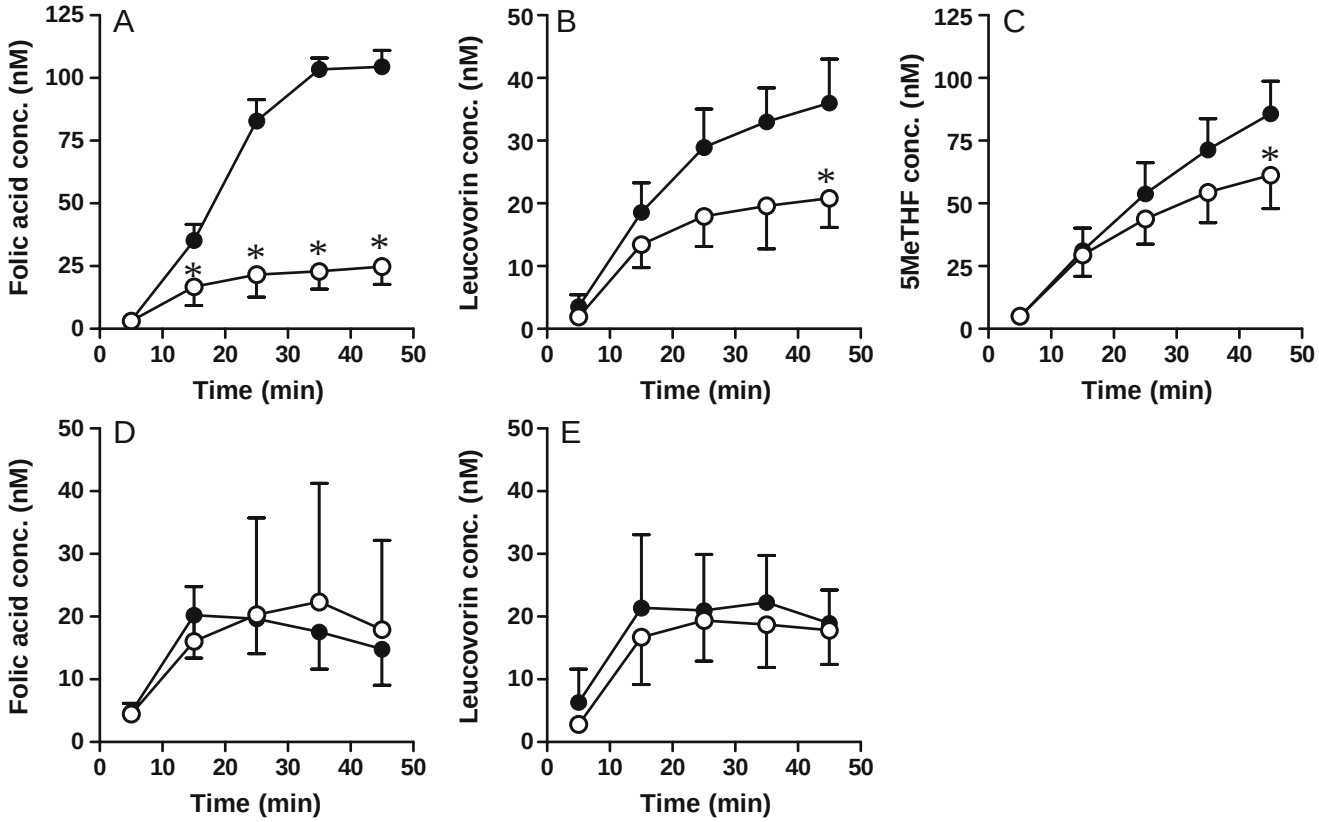

Fig. 3. Mucosal-to-serosal transport of folates in everted sacs from intestines. Everted segments of the duodenum (**A**–**C**) or jejunum (**D**, **E**) of wild-type and *Mrp3*$^{-/-}$ mice were incubated with folic acid (**A**, **D**), leucovorin (**B**, **E**), or 5MeTHF (**C**). One type of folate was added to the mucosal buffer to a final concentration of 5 μM. The serosal side was perfused with drug-free buffer, and the total volume of serosal perfusate was collected every 10 min. Concentrations were determined in the serosal perfusate in the everted sacs of the wild-type (*filled circle*) and *Mrp3*$^{-/-}$ (*white circle*) mice. Each point represents the mean±SD (n=3 or 4). *P<0.05, significantly different from wild-type mice.

levels of these transcripts between the wild-type and *Mrp3*$^{-/-}$ mice, although some statistically significant differences were occasionally found.

DISCUSSION

In this study, we investigated the importance of Mrp3 in the intestinal absorption of folates using *Mrp3*$^{-/-}$ mice. Folates are a water-soluble vitamin, efficiently absorbed from the intestine by active transport systems. The molecular entity involved in the basolateral efflux transport is yet to be identified, although apical uptake transporters have been extensively explored.

Following oral administration of folic acid, *Mrp3*$^{-/-}$ mice exhibited significantly lower C_{max} and AUC values for folic acid than those of wild-type mice (Fig. 1A), whereas the rate of systemic elimination of folic acid was similar in the two strains (Fig. 1B). Considering the fact that $CL_{tot,p}$ was lower than the hepatic blood flow rate (106 mL/min/kg) (19), the hepatic first pass effect is negligible in both wild-type and *Mrp3*$^{-/-}$ mice for folic acid. Accordingly, the lower C_{max} and AUC in *Mrp3*$^{-/-}$ mice are attributable to lower intestinal absorption. In addition to folic acid, the absorption of leucovorin into the systemic circulation was significantly delayed in *Mrp3*$^{-/-}$ mice compared with wild-type mice (Fig. 2), although the impact of Mrp3 dysfunction was not so marked compared with folic acid.

To support the *in vivo* results, the mucosal-to-serosal transport of folic acid was determined using everted sacs from mouse duodenum and jejunum. As observed for methotrexate (7), the mucosal-to-serosal transport (PS_{net}) of folic acid was markedly higher in the duodenum than in jejunum, presumably because of the abundant expression of uptake transporters in the duodenum (7). The intrinsic transport activity in the mucosal-to-serosal transport (PS_{net}) of folic acid was significantly lower in the duodenum of *Mrp3*$^{-/-}$ mice than in that of wild-type mice. Simultaneously, the tissue concentration (C_{sac}) of folic acid was increased in the duodenal sacs from *Mrp3*$^{-/-}$ mice, indicating that the lower PS_{net} in *Mrp3*$^{-/-}$ mice is not attributable to a reduction in mucosal uptake but to a reduction in net efflux from inside the cells. Actually, the serosal efflux ($PS_{serosal}$) of folic acid was markedly lower in the duodenum of *Mrp3*$^{-/-}$ mice compared with that in wild-type mice. Mrp3 accounts for the major part of the basolateral efflux of folic acid in the duodenum. Previously, Na^+-independent uptake was demonstrated in the BLMVs for folic acid (16, 17). Since the K_m value of folic acid (0.7 μM) determined in the BLMVs from rat jejunum (20) was greater than the C_{sac} of folic acid (0.3 μM) in the duodenum of wild-type mice, it is unlikely that the contribution of the transporter was underestimated because of saturation. Unlike the duodenum, neither PS_{net} nor C_{sac} was affected by a defect of Mrp3 function in the jejunum, although Mrp3 is expressed throughout the entire

Table II. Permeability Surface Area Products and Tissue Concentrations of Folates in Intestinal Everted Sacs Prepared from Wild-type and *Mrp3*$^{-/-}$ Mice

		Wild-type	*Mrp3*$^{-/-}$
PS_{net} (μL/min/sac)			
Folic acid	duodenum	2.09±0.13	0.497±0.143*
	jejunum	0.296±0.115	0.359±0.285
Leucovorin	duodenum	0.721±0.140	0.416±0.093*
	jejunum	0.379±0.107	0.356±0.109
5MeTHF	duodenum	1.72±0.26	1.23±0.27*
C_{sac} (μM)			
Folic acid	duodenum	0.291±0.153	1.17±0.49*
	jejunum	0.0768±0.0294	0.123±0.048
Leucovorin	duodenum	0.655±0.040	1.76±0.37*
	jejunum	0.216±0.042	0.382±0.104
5MeTHF	duodenum	6.30±1.91	7.88±1.63
$PS_{serosal}$ (μL/min/sac)			
Folic acid	duodenum	41.6±16.8	2.62±1.95*
Leucovorin	duodenum	5.56±1.44	1.23±0.45*
5MeTHF	duodenum	1.47±0.52	0.784±0.194*

Folates were added to the mucosal buffer to a final concentration of 5 μM. Tissue concentration (C_{sac}) was determined at 50 min. The permeability–surface area products for the net transport from the mucosal side to the serosal side (PS_{net}) and across the serosal membrane ($PS_{serosal}$) were calculated by dividing the transport rate at 40–50 min by the concentration in the mucosal medium (5 μM) and the tissue concentration (C_{sac}), respectively. Each value represents the mean±SD (n=3 or 4). *P<0.05, significantly different from wild-type mice.

length of the intestine (2,7). This contradiction is probably attributable to the low contribution of the transcellular pathway to the net mucosal-to-serosal transport of folic acid in the jejunal everted sacs. This is supported by the fact that 1) PS_{net} was seven-fold lower in the jejunum than in the duodenum, 2) the C_{sac} of folic acid was lower in the jejunum than in the duodenum, and 3) the PS_{net} of folic acid is similar to that of methotrexate in the jejunum, which seemed to be mediated by the paracellular pathway (7).

The PS_{net} of leucovorin was reduced by the impairment of Mrp3 in the duodenum, where the $PS_{serosal}$ of leucovorin was markedly reduced, showing that most of the basolateral efflux of leucovorin in the duodenum is mediated by Mrp3. In contrast, PS_{net} of lecuovorin was similar in the jejunum of wild-type and *Mrp3*$^{-/-}$ mice. Since leucovorin is a potential substrate of Pcft (21), the contribution of transcellular pathway may not be large enough in the jejunum to detect the effect of Mrp3 impairment. Actually, PS_{net} in the jejunum of leucovorin was similar to that of folic acid. Although Mrp3 plays a significant role in the serosal efflux of leucovorin in the duodenum, the impact of Mrp3 impairment on the systemic exposure of leucovorin was less remarkable compared with that of folic acid. Because the PS_{net} of leucovorin in the duodenum was only one-third of that of folic acid in the wild-type mice, it is possible that the fraction of leucovorin absorbed during its transit through the duodenum, where Mrp3 plays a significant role, is lower than that of folic acid, resulting in a lower impact of Mrp3 *in vivo*.

Unlike folic acid and leucovorin, Mrp3 impairment had only a marginal impact on the mucosal-to-serosal transport of 5MeTHF in the duodenum (Fig. 3). Actually, the contribution of Mrp3 to the basolateral efflux of 5MeTHF was at most 50% based on the reduction of $PS_{serosal}$ (Table II). Considering the hydrophilic nature of 5MeTHF, it is highly possible that the serosal efflux remaining in *Mrp3*$^{-/-}$ mice involves transporter(s). The regional difference in the mucosal-to-serosal transport of 5MeTHF along the intestine remains to be examined. However, the fact that 5MeTHF is a substrate of Pcft (21–23) suggests that the PS_{net} of 5MeTHF exhibits a regional difference as observed in the case of folic acid and leucovorin.

To examine the possibility that defect of Mrp3 perturbs folate homeostasis, we determined endogenous levels of 5MeTHF, vitamin B_{12}, and homocysteine in the plasma of wild-type and *Mrp3*$^{-/-}$ mice. 5MeTHF and vitamin B_{12} are involved in the metabolism of homocysteine, a sulfur-containing amino acid produced by the conversion of methionine. Folate fortification reduces plasma homocysteine levels, and its combined supplementation with vitamin B_{12} enhances this effect (24). Plasma concentrations of 5MeTHF, vitamin B_{12}, and homocysteine were not affected by defect of Mrp3 (Fig. 4), and only minimal differences in the mRNA levels of enzymes involved in folate homeostasis were observed in the wild-type and *Mrp3*$^{-/-}$ mice (Fig. 5). These results indicate that folate

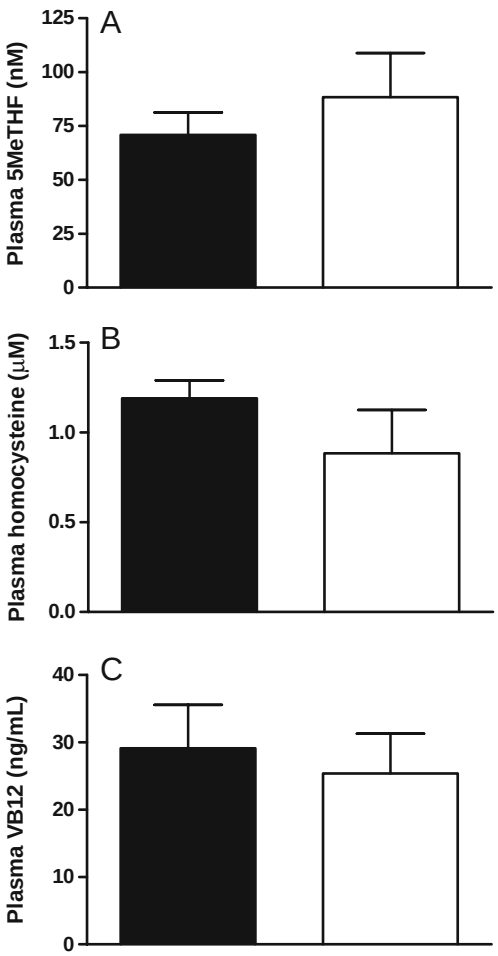

Fig. 4. Plasma levels of 5MeTHF, homocysteine, and vitamin B_{12} in wild-type and *Mrp3*$^{-/-}$ mice. Plasma concentrations of endogenous 5MeTHF (**A**), homocysteine (**B**), and vitamin B_{12} (**C**) in wild-type (closed columns) and *Mrp3*$^{-/-}$ (*open columns*) mice were determined. Each column represents the mean±SD (n=3 or 4). No significant differences were observed between the wild-type and *Mrp3*$^{-/-}$ mice.

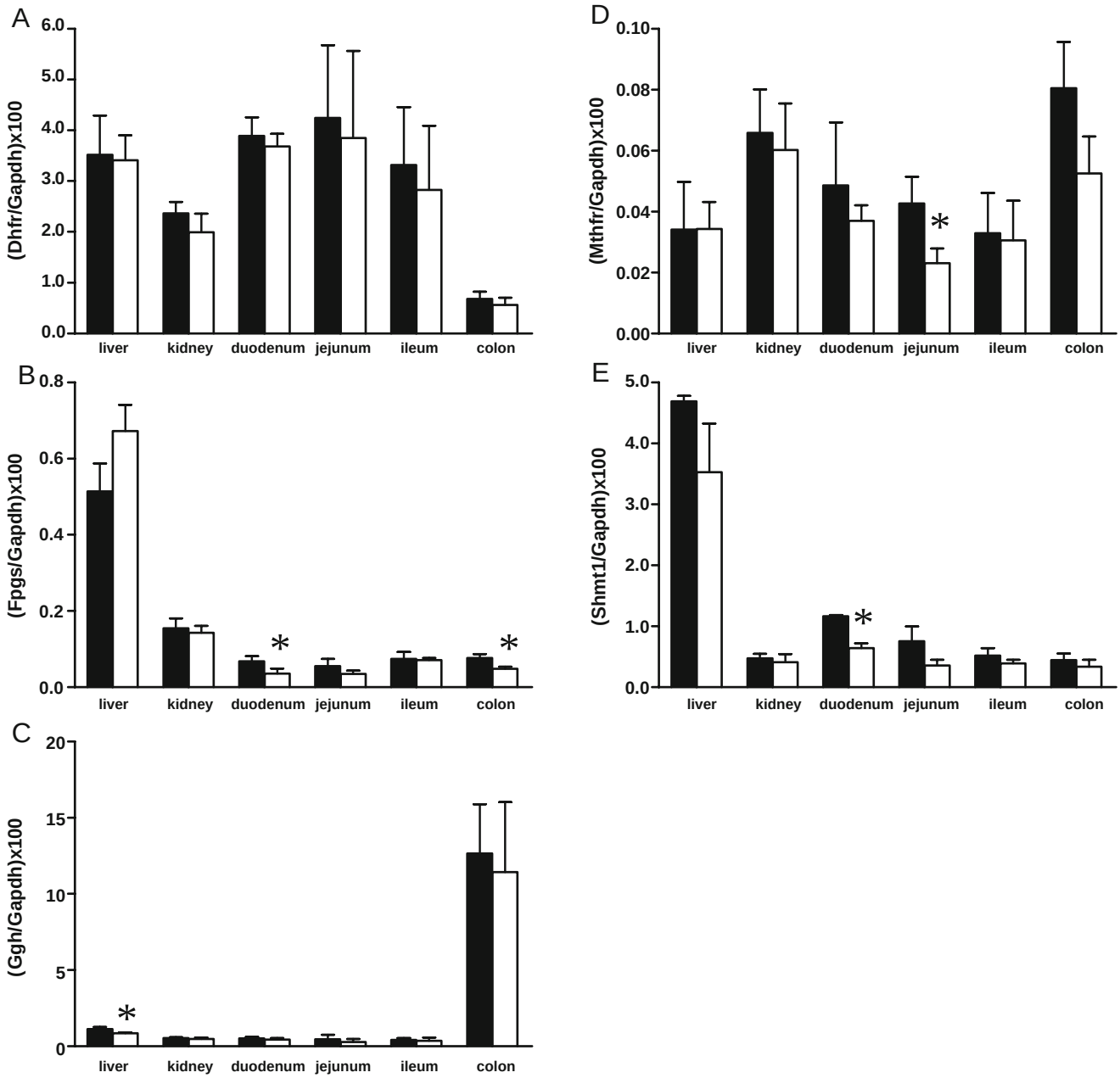

Fig. 5. mRNA expression of enzymes related to folate homeostasis in the livers, in the kidneys, and along the intestines of wild-type and *Mrp3*$^{-/-}$ mice. mRNA expression of Dhfr (**A**), Fpgs (**B**), Ggh (**C**), Mthfr (**D**), and Shmt1 (**E**) in wild-type (*closed columns*) and *Mrp3*$^{-/-}$ (*open columns*) mice was quantified by real-time PCR and was normalized to that of Gapdh. Each column represents the mean±SD (n=3). * P<0.05, significantly different from wild-type mice.

homeostasis is maintained in *Mrp3*$^{-/-}$ mice at least under normal conditions. Presumably, this may be ascribed to the serosal efflux by unknown transporter, which prevents diminishing transepithelial transport of 5MeTHF by the defect of Mrp3 function.

Generally, ABC transporters involved in xenobiotic detoxification, such as Mrp2, Bcrp, and P-glycoprotein, are expressed in the apical membranes of polarized cells, and they facilitate the systemic elimination of xenobiotics into the adjacent luminal space (25). Mrp3 has been considered to be a part of the mechanism of xenobiotic detoxification. Actually, it mediates the basolateral efflux of glucuronide conjugates of xenobiotics from the liver and small intestine into the systemic circulation (26,27). Mrp3 becomes a particularly important pathway when biliary excretion is impaired, preventing the accumulation of xenobiotic metabolites in the liver. This study reports, for the first time, that Mrp3 is involved in the transport of essential nutrients in the body in conjunction with folate uptake transporters in mouse. Malabsorption of folate caused by mutation of PCFT indicates that transcellular transport is a major pathway in the intestinal absorption of folate in humans. Since hMRP3 is expressed in the intestine (28) and accepts folates as substrates, it is possible that MRP3 also plays a significant role in the folate absorption in humans. Furthermore, considering its broad substrate specificity, Mrp3 may mediate

the intestinal absorption of other compounds. This should be examined in future studies.

CONCLUSION

Mrp3 mediates the serosal efflux of folates, thereby, facilitating their intestinal absorption together with uptake transporters in mouse duodenum, but defect of Mrp3 does not disrupt folate homeostasis.

ACKNOWLEDGMENTS

We would like to thank Dr. Piet Borst (The Netherlands Cancer Institute, Amsterdam, The Netherlands) for supplying the *Mrp3*$^{-/-}$ mice. This work was supported by Grant-in-Aid for Scientific Research (A) (20249008) from the Ministry of Education, Culture, Sports, Science and Technology (MEXT).

REFERENCES

1. Hirohashi T, Suzuki H, Ito K, Ogawa K, Kume K, Shimizu T, *et al*. Hepatic expression of multidrug resistance-associated protein-like proteins maintained in eisai hyperbilirubinemic rats. Mol Pharmacol. 1998;53:1068–75.
2. Zelcer N, van de Wetering K, de Waart R, Scheffer GL, Marschall HU, Wielinga PR, *et al*. Mice lacking Mrp3 (Abcc3) have normal bile salt transport, but altered hepatic transport of endogenous glucuronides. J Hepatol. 2006;44:768–75.
3. Donner MG, Keppler D. Up-regulation of basolateral multidrug resistance protein 3 (Mrp3) in cholestatic rat liver. Hepatology. 2001;34:351–9.
4. Zelcer N, van de Wetering K, Hillebrand M, Sarton E, Kuil A, Wielinga PR, *et al*. Mice lacking multidrug resistance protein 3 show altered morphine pharmacokinetics and morphine-6-glucuronide antinociception. Proc Natl Acad Sci USA. 2005;102:7274–9.
5. Scheffer GL, Kool M, Heijn M, de Haas M, Pijnenborg AC, Wijnholds J, *et al*. Specific detection of multidrug resistance proteins MRP1, MRP2, MRP3, MRP5, and MDR3 P-glycoprotein with a panel of monoclonal antibodies. Cancer Res. 2000;60:5269–77.
6. Kusuhara H, Sugiyama Y. *In vitro-in vivo* extrapolation of transporter-mediated clearance in the liver and kidney. Drug Metab Pharmacokinet. 2009;24:37–52.
7. Kitamura Y, Hirouchi M, Kusuhara H, Schuetz JD, Sugiyama Y. Increasing systemic exposure of methotrexate by active efflux mediated by multidrug resistance-associated protein 3 (mrp3/abcc3). J Pharmacol Exp Ther. 2008;327:465–73.
8. Matsushima S, Maeda K, Hayashi H, Debori Y, Schinkel AH, Schuetz JD, *et al*. Involvement of multiple efflux transporters in hepatic disposition of fexofenadine. Mol Pharmacol. 2008;73:1474–83.
9. Rost D, Mahner S, Sugiyama Y, Stremmel W. Expression and localization of the multidrug resistance-associated protein 3 in rat small and large intestine. Am J Physiol Gastrointest Liver Physiol. 2002;282:G720–6.
10. Hirohashi T, Suzuki H, Takikawa H, Sugiyama Y. ATP-dependent transport of bile salts by rat multidrug resistance-associated protein 3 (Mrp3). J Biol Chem. 2000;275:2905–10.
11. Dawson PA, Hubbert M, Haywood J, Craddock AL, Zerangue N, Christian WV, *et al*. The heteromeric organic solute transporter alpha-beta, Ostalpha-Ostbeta, is an ileal basolateral bile acid transporter. J Biol Chem. 2005;280:6960–8.
12. Sakamoto S, Suzuki H, Kusuhara H, Sugiyama Y. Efflux mechanism of taurocholate across the rat intestinal basolateral membrane. Mol Pharm. 2006;3:275–81.
13. Zeng H, Chen ZS, Belinsky MG, Rea PA, Kruh GD. Transport of methotrexate (MTX) and folates by multidrug resistance protein (MRP) 3 and MRP1: effect of polyglutamylation on MTX transport. Cancer Res. 2001;61:7225–32.
14. Liu M, Ge Y, Cabelof DC, Aboukameel A, Heydari AR, Mohammad R, *et al*. Structure and regulation of the murine reduced folate carrier gene: identification of four noncoding exons and promoters and regulation by dietary folates. J Biol Chem. 2005;280:5588–97.
15. Qiu A, Jansen M, Sakaris A, Min SH, Chattopadhyay S, Tsai E, *et al*. Identification of an intestinal folate transporter and the molecular basis for hereditary folate malabsorption. Cell. 2006;127:917–28.
16. Dudeja PK, Kode A, Alnounou M, Tyagi S, Torania S, Subramanian VS, *et al*. Mechanism of folate transport across the human colonic basolateral membrane. Am J Physiol Gastrointest Liver Physiol. 2001;281:G54–60.
17. Said HM, Redha R. A carrier-mediated transport for folate in basolateral membrane vesicles of rat small intestine. Biochem J. 1987;247:141–6.
18. Enokizono J, Kusuhara H, Sugiyama Y. Regional expression and activity of breast cancer resistance protein (Bcrp/Abcg2) in mouse intestine: overlapping distribution with sulfotransferases. Drug Metab Dispos. 2007;35:922–8.
19. Brown RP, Delp MD, Lindstedt SL, Rhomberg LR, Beliles RP. Physiological parameter values for physiologically based pharmacokinetic models. Toxicol Ind Health. 1997;13:407–84.
20. Kumar CK, Nguyen TT, Gonzales FB, Said HM. Comparison of intestinal folate carrier clone expressed in IEC-6 cells and in Xenopus oocytes. Am J Physiol. 1998;274:C289–94.
21. Nakai Y, Inoue K, Abe N, Hatakeyama M, Ohta KY, Otagiri M, *et al*. Functional characterization of human proton-coupled folate transporter/heme carrier protein 1 heterologously expressed in mammalian cells as a folate transporter. J Pharmacol Exp Ther. 2007;322:469–76.
22. Zhao R, Min SH, Qiu A, Sakaris A, Goldberg GL, Sandoval C, *et al*. The spectrum of mutations in the PCFT gene, coding for an intestinal folate transporter, that are the basis for hereditary folate malabsorption. Blood. 2007;110:1147–52.
23. Qiu A, Min SH, Jansen M, Malhotra U, Tsai E, Cabelof DC, *et al*. Rodent intestinal folate transporters (SLC46A1): secondary structure, functional properties, and response to dietary folate restriction. Am J Physiol Cell Physiol. 2007;293:C1669–78.
24. Ubbink JB, Vermaak WJ, van der Merwe A, Becker PJ, Delport R, Potgieter HC. Vitamin requirements for the treatment of hyperhomocysteinemia in humans. J Nutr. 1994;124:1927–33.
25. Ito K, Suzuki H, Horie T, Sugiyama Y. Apical/basolateral surface expression of drug transporters and its role in vectorial drug transport. Pharm Res. 2005;22:1559–77.
26. Zamek-Gliszczynski MJ, Nezasa K, Tian X, Bridges AS, Lee K, Belinsky MG, *et al*. Evaluation of the role of multidrug resistance-associated protein (Mrp) 3 and Mrp4 in hepatic basolateral excretion of sulfate and glucuronide metabolites of acetaminophen, 4-methylumbelliferone, and harmol in Abcc3−/− and Abcc4−/− mice. J Pharmacol Exp Ther. 2006;319:1485–91.
27. Kitamura Y, Kusuhara H, Sugiyama Y. Functional characterization of multidrug resistance-associated protein 3 (Mrp3/Abcc3) in the basolateral efflux of glucuronide conjugates in the mouse small intestine. *J Pharmacol Exp Ther*, in press.
28. Taipalensuu J, Tornblom H, Lindberg G, Einarsson C, Sjoqvist F, Melhus H, *et al*. Correlation of gene expression of ten drug efflux proteins of the ATP-binding cassette transporter family in normal human jejunum and in human intestinal epithelial Caco-2 cell monolayers. J Pharmacol Exp Ther. 2001;299:164–70.